High-Speed Measurement of Sound-Flow Interaction at Perforated Liners with Bias Flow

Daniel Haufe[1], André Döring[1], Anita Schulz[2], Friedrich Bake[2],
Lars Enghardt[2,3], Jürgen Czarske[1] und Andreas Fischer[1]

[1] *TU Dresden, 01062 Dresden, Deutschland, Email: daniel.haufe@tu-dresden.de*

[2] *German Aerospace Center (DLR), 10623 Berlin, Deutschland, Email: anita.schulz@dlr.de*

[3] *TU Berlin, 10623 Berlin, Deutschland*

Introduction

In order to experimentally investigate the interaction between sound and flow occurring e.g. in the thermoacoustic effect [1], in the case of acoustic streaming [2] or in aeroacoustics [3], a contactless high-speed measurement of the fluid velocity vector is required for the time-resolved acquisition of the sound field and the flow field. Consequently, a high measurement rate within the kHz range is required to ascertain deterministic and stochastic oscillations corresponding to the acoustic velocity and to flow turbulence terms. Furthermore, a volumetric measurement is demanded, when complex sound fields or flow turbulence structures are of interest.

In this article, we present a laser measurement methodology which fulfills these challenging requirements. As a result, a measurement rate of maximum 100 kHz is achieved using fast photodetectors, e.g. a high-speed camera, and a volumetric measurement is accomplished. In addition, the methodology is applied to the analysis of the sound-flow interaction of aeracoustic damping phenomena at a perforated liner with bias flow in order to achieve a deeper understanding of the damping mechanism regarding the aspired increase of the damping efficiency.

Methodology

In order to analyze the sound-flow interaction at a perforated liner, two approaches using a laser optical measurement method are followed for the acquisition of the velocity field $\vec{v}$ using seeding particles as tracers. The particles follow the fluid, assuming slip is negligible [4, p. 253]. Here, the Doppler global velocimetry with sinusoidal laser frequency modulation (FM-DGV) based on [5] is used. For the FM-DGV measurement, a laser (type *TOPTICA TA-100*) with a light wavelength $\lambda = 895\,\text{nm}$ is employed for the illumination of the particles from the $\vec{i}$-direction, see Figure 1a. The laser frequency is modulated sinusoidally, with a modulation frequency that equals the maximum measurement rate and typically amounts to 100 kHz. The laser light is scattered by the particles, whereby the frequency of the light is shifted by the Doppler frequency

$$f_{\mathrm{D},k} = \frac{\vec{o}_k - \vec{i}}{\lambda}\vec{v} = \frac{\left|\vec{o}_k - \vec{i}\right|}{\lambda} v_k, \qquad (1)$$

depending on the direction $\vec{o}_k$ of the observation that determines the velocity component v_k to be measured [6].

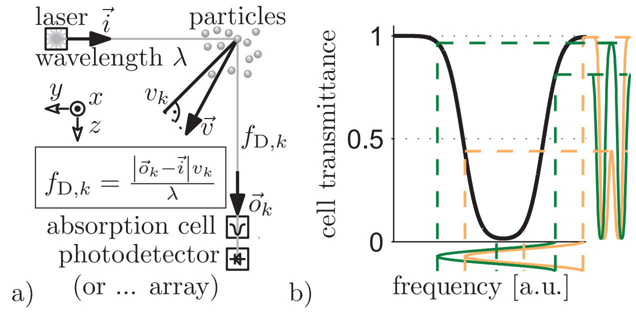

Figure 1: a) principle of the fluid velocity measurement using FM-DGV employing a spectroscopic evaluation of the Doppler frequency and b) frequency-intensity-conversion using the non-linear transmittance of a cesium absorption cell in case of two different Doppler frequencies

In order to obtain the Doppler frequency, the scattered light is observed through an absorption cell being used as a frequency-to-intensity converter with a non-linear transfer function, see Figure 1b. Thus, the transmitted intensity is modulated and contains harmonics that depend on the Doppler frequency. The intensity is detected by a fast photodetector and the detector signal is evaluated in the frequency domain. The quotient of the signal amplitudes at the first and at the second harmonic of the modulation frequency is independent of the scattered light power and yields, after calibration, the velocity component v_k.

In the first approach, three velocity components $v_k, k = 1 \ldots 3$ are measured in parallel at a measurement rate of 100 kHz, employing three observation units in different directions $\vec{o}_k$. To ascertain the velocity vector $\vec{v}$, the components v_k are transformed into Cartesian coordinates using a matrix operation adapted from [7]. To get a volumetric velocity field, a linear array of eight avalanche photodiodes (bandwidth of about 400 kHz) is orientated along the y-direction at each observation unit and traversed to eight positions in both x- and z-direction. Thereby, the traversing stage is coupled with the laser beam to traverse the illumination unit synchronously with the observation unit. The resulting cubic measurement region has $8^3 = 512$ measurement locations.

In the second approach, the number of measurement locations is increased without augmenting the number of traversing steps. For that purpose, a high-speed camera, type *Phantom v1610* (maximum 1 million frames per second), is used as photodetector. This measurement is performed with FM-DGV using the same setup as in Figure 1a, i.e. with one observation unit directed in the positive z-direction. Consequently, one velocity component v_1 is measured, which is oblique in the y- and z-direction. To obtain the Cartesian velocity components v_y and v_z, a second measurement of the component v_2 at the same location is performed with the opposite observation direction, i.e. in the negative z-direction. Finally both obtained velocity components are transformed into Cartesian coordinates as described before at the first approach. In addition, a successive traversing in the z-direction of both laser light illumination and observation unit is performed in order to obtain the volumetric velocity field sequentially.

Setup

The sound-flow interaction is experimentally investigated at a generic perforated liner installed in a test rig (inspired by [3]) that represents a duct with rectangular cross section (80 mm × 60 mm, cut-off frequency: 2.1 kHz) having glass windows at three sides to provide access for the optical measurements. The liner perforation consists of a 1 mm thick facing sheet with 53 regularly arranged circular orifices (diameter: 2.5 mm), as depicted in Figure 2. The point of origin is at the center of the central

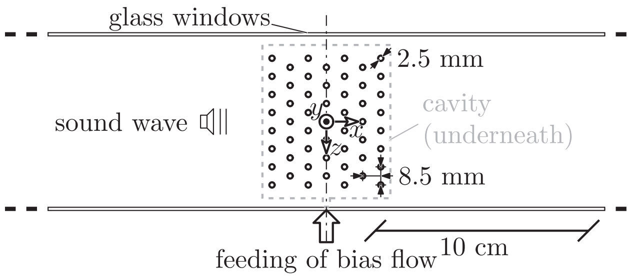

Figure 2: sketch of the setup: perforated liner and single-volume cavity where the bias flow charged with seeding particles is fed into, installed in the test rig with glass windows providing optical access for the measurements

orifice. To enhance the damping performance, a bias flow is driven through the orifices at a controlled mass rate of 5 kg/h. Underneath the perforation is a single-volume cavity (dimensions in x, y, z: 60 mm × 49 mm × 72 mm), where the bias flow is fed into, charged with seeding particles (diethylhexyl sebacate, diameter: ca. 1 µm, generator type: *PIVpart14*). Apart from the bias flow, a small suction flow is present to avoid an overfill with particles. An acoustic plane wave is excited by a speaker, type *MONACOR KU-516*, at a frequency of 1122 Hz where the damping performance of the liner is maximum (dissipation coefficient ≈ 60 %, measured using microphones according to [3]). The resulting sound pressure level is about 120 dB, measured by a flush-mounted condenser microphone at the outermost x-position. The experiments are conducted at ambient conditions.

For the FM-DGV measurements, the laser light illumination is in negative y-direction. In the first approach, using three observation units (each with one photodiode array), the three observation directions are $\vec{o}_1 = (\sin[35°], 0, \cos[35°])$, $\vec{o}_2 = (-\sin[35°], 0, -\cos[35°])$ and $\vec{o}_3 = (\sin[35°], 0, -\cos[35°])$; the measurement rate amounts to 100 kHz. In the second approach, using the high-speed camera, a light sheet in the xy-plane is set up and the observation direction is $\vec{o}_1 = (0, 0, 1)$ and $\vec{o}_2 = (0, 0, -1)$, respectively. Since the image resolution of the camera decreases for higher frame rates, a trade-off between both is necessary. Hence, the frame rate of 100 kHz at an image resolution of 128 px × 128 px is chosen. To achieve oversampling by at least factor four (regarding the second order harmonic of the modulation frequency) with the camera, the modulation frequency, that equals the measurement rate, is set to 10 kHz.

Results

(a) FM-DGV using photodiode arrays

For the investigation of the sound-flow interaction, the acoustically induced oscillation velocity $\vec{v}_{osc}$, i.e. the zero-mean velocity that changes with the acoustic excitation frequency (including the acoustic particle velocity) is considered at first. For that purpose, the magnitude v_{osc} of the velocity vector is depicted in Figure 3 for a variable phase angle φ, near the central orifice at the central xy-plane, i.e. $z = 0$, as an example. The uncertainty of v_{osc}

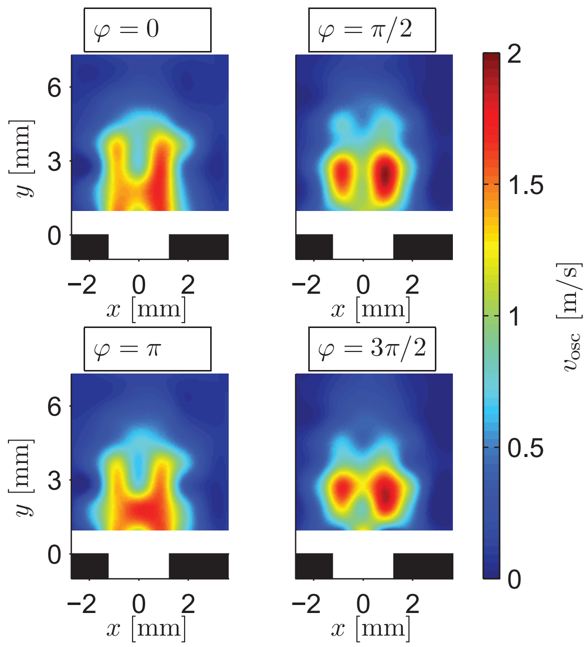

Figure 3: phase-resolved magnitude $v_{osc}(\varphi)$ of the oscillation velocity field (interpolated), measured with FM-DGV at $z = 0$ near the central orifice of the generic perforated liner from Figure 2 with a bias flow (mass rate 5 kg/h, dissipation coefficient 60 %) at the sound excitation frequency of 1122 Hz, the black boxes indicate the rim of the orifice

is about 1 mm/s, using averaging for a measurement duration of 80 s. The spatial resolution of the measurement is about 800 µm. For the sake of clarity, a cubic interpolation is used in Figure 3. The maximum value of v_{osc} is reached adjacent to (left in Figure 3) or above (right in

Figure 3) the rims of the orifice, respectively. The magnitude of the oscillation velocity vector amounts up to 2 m/s, which is presumably dominated by an acoustically induced flow, according to [3]. It has been reported e.g. in [8] that this induced flow contains vortices. In order to check for acoustically induced vortices, the vorticity

$$\vec{\omega} = \vec{\nabla} \times \vec{v} \tag{2}$$

of the velocity field is calculated. Since the rotation of acoustic particle velocity field is typically zero [9, p. 44], solely the flow vorticity is observed here. Due to the vector calculus, the volumetric velocity data has to be taken into account. The resulting magnitude ω of the vorticity vector is depicted in Figure 4 as an isosurface plot for a variable phase angle φ with respect to the sound excitation frequency. In the figure, the creation of a doughnut

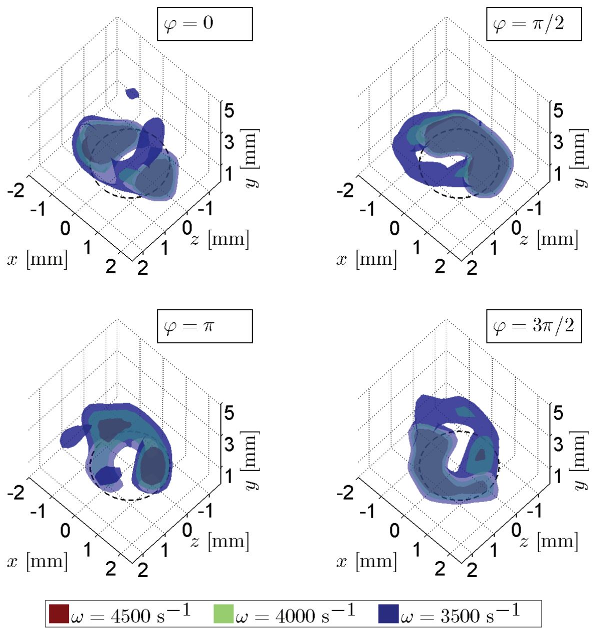

Figure 4: isosurface plots (interpolated) of the phase-resolved vorticity magnitude $\omega(\varphi)$ of the velocity field, measured with FM-DGV at the central orifice of the generic perforated liner from Figure 2 with a bias flow (mass rate 5 kg/h, dissipation coefficient 60 %) at the sound excitation frequency of 1122 Hz, the dashed circle indicates the rim of the orifice

structure around the central orifice is apparent, which gradually ascents in the positive y-direction. This means that the interaction of the sound wave with the bias flow initiates ring vortices that detach from the perforation. According to the theory of [10], the vortices break up, loose energy and finally dissipate into heat. Since a large amount of acoustic energy is damped for this liner configuration, it is assumed that the energy initially contained in the vortices has been extracted from the incoming acoustic wave and transferred to the flow.

To investigate this potential energy transfer in more detail, a spectral analysis has been accomplished. For that purpose, the power spectral density (PSD) of the velocity $\vec{v}$ is calculated based on the sum of the periodograms of the measured velocity time series for the three Cartesian velocity components v_x, v_y and v_z. The resulting PSD (corresponding to the spectrum of the kinetic energy) is depicted in Figure 5 as an example for the position $(x, y, z) = (-1.8\,\mathrm{mm}, 2.8\,\mathrm{mm}, 0\,\mathrm{mm})$ which is above the rim of the central orifice. In comparison with the configuration without sound excitation, there is a broadband PSD gain. In addition, there are distinct peaks at the excitation frequency and at their harmonics. Hence, a nonlinear behavior is present which might either result from the liner, from the loudspeaker or a combination of both. Apart from that, there is also a PSD gain close-by the excitation frequency (and their harmonics). It is supposed that this corresponds to flow structures with various length scales (related to corresponding frequencies) which are initiated by the sound-flow interaction. Former experiments with variable excitation frequencies indicated that there is a correlation between the dissipation coefficient of the liner and the PSD gain of the velocity, see e.g. [11]. The results obtained there and here support the hypothesis that flow vortex generation induced by the sound-flow interaction is predominantly responsible for the acoustic damping at bias flow liners.

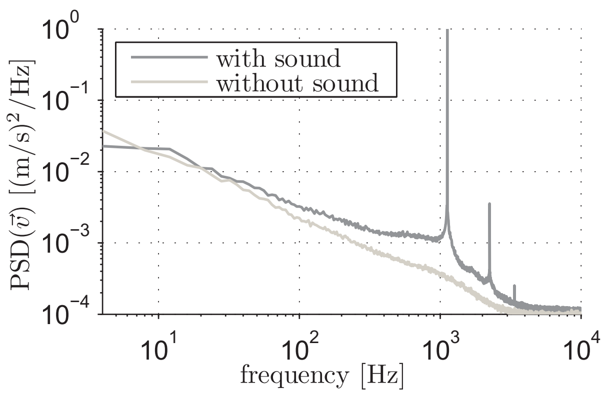

Figure 5: power spectral density (PSD) of the velocity $\vec{v}$ at $(x, y, z) = (-1.8\,\mathrm{mm}, 2.8\,\mathrm{mm}, 0\,\mathrm{mm})$ near the central orifice of the generic perforated liner from Figure 2 with a bias flow (mass rate 5 kg/h, dissipation coefficient 60 %) at the sound excitation frequency of 1122 Hz, measured with FM-DGV

(b) FM-DGV using a high-speed camera

To allow the instantaneous two-dimensional acquisition of the velocity field by imaging of the scattered light, the applicability of a high-speed camera for FM-DGV is shown for the first time. The resulting phase-resolved oscillation velocity $v_{\mathrm{osc,y}}$ in the y-direction at the sound excitation frequency is depicted in Figure 6 as an example for $z = -1.8\,\mathrm{mm}$ near the central orifice of the liner. The uncertainty of the velocity amplitude is about 1 mm/s, using averaging for a measurement duration of 90 s. The area of measurement comprises $32^2 = 1024$ locations where the velocity is measured in parallel. Since the spatial resolution is sufficient here (about 250 µm), no interpolation is applied. A single-pixel resolution is also possible (which in turn raises the number of measurement locations) when the currently used software binning of 4 px × 4 px (to reduce the evaluation effort considering the enormous raw data rate of about three gigabyte per

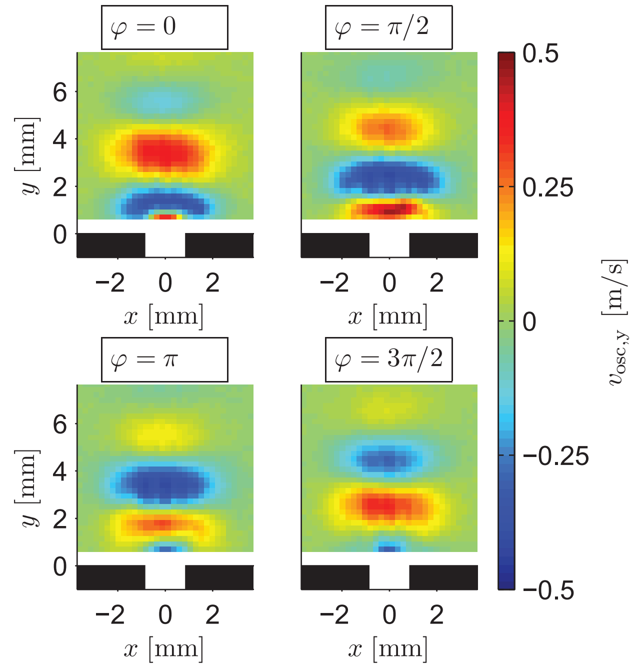

Figure 6: phase-resolved velocity $v_{\mathrm{osc,y}}$ (φ) in the y-direction (w./o. interpolation) near the central orifice of the generic perforated liner from Figure 2 with bias flow (mass rate 5 kg/h, dissipation coefficient 60 %) at the sound excitation frequency of 1122 Hz, measured with FM-DGV at $z = -1.8$ mm using a high-speed camera with a spatial resolution of about 250 µm

second) is omitted. In Figure 6, the amplitude of $v_{\mathrm{osc,y}}$ has its maximum value of about 0.5 m/s near the perforation. The velocity structure repeats in y-direction within an interval of about 4 mm corresponding to a propagation speed of about 5 m/s which is not equivalent to the speed of sound, but equals approximately the estimated velocity of the bias flow. Consequently, this again indicates a detachment of flow vortices. The future aim is to acquire the complete velocity vector information by implementing an additional particle image velocimetry (PIV) evaluation [4], using the estimated particle displacement in the xy-plane between two subsequent images and the known time interval in between. Then, the simultaneous measurement of the velocity vector field is accomplished, allowing two-dimensional correlation, especially of stochastic velocity fluctuations, e.g. for advanced analysis of the damping phenomena at liners.

Summary & Outlook

We demonstrate high-speed measurements of velocity vector fields in fluids using two laser measurement approaches which allow resolving the interaction of sound and flow. As an example, the acoustic damping at a perforated liner with bias flow is investigated, where acoustically induced flow vortices are resolved volumetrically, for the first time also using a high-speed camera. The experimental investigations reveal ring vortex structures that detach from the perforation and eventually dissipate. Due to the high measurement rate of up to 100 kHz, a spectral analysis of the velocity is additionally performed where a sound induced broadband PSD gain for the velocity is observed. These results support former hypotheses that the damping performance of the liner is correlated to the vortex production. Future work will focus on the establishment of an energy balance from the acoustic to the flow field to better understand the acoustic damping in order to optimize efficiency of the liner.

Acknowledgment

The authors thank the German Research Foundation (DFG) for the funding of the projects CZ 55/25-1 and EN 797/2-1. Raimund Schlüßler is gratefully acknowledged for his supporting work.

References

[1] Berson, A. et al.: Measurement of acoustic velocity in the stack of a thermoacoustic refrigerator using particle image velocimetry. Heat and Mass Transfer 44 (2008), 1015–1023

[2] Castrejón-Pita, J. R. et al.: Experimental demonstration of the Rayleigh acoustic viscous boundary layer theory. Physical Review E 73 (2006), 036601–1–036601–5

[3] Heuwinkel, C. et al.: Characterization of a Perforated Liner by Acoustic and Optical Measurements. 16$^{\mathrm{th}}$ AIAA/CEAS Aeroacoustics Conference, 2010-3765, Stockholm, Sweden, 2010

[4] Raffel, M. et al.: Particle Image Velocimetry: A Practical Guide. Springer, Berlin, Heidelberg, New York, 1998

[5] Fischer, A. et al.: Investigation of time-resolved single detector Doppler global velocimetry using sinusoidal laser frequency modulation. Measurement Science and Technology 18 (2007), 2529–2545

[6] Goldstein, R. J. et al.: Measurement of Laminar Flow Development in a Square Duct Using a Laser-Doppler Flowmeter. Journal of Applied Mechanics – Transactions of the ASME 34 (1967), 813–818

[7] Charrett, T. O. H. et al.: Investigation into the selection of viewing configurations for three-component planar Doppler velocimetry measurements. Applied Optics 46 (2007), 4102–4116

[8] Rupp, J. et al.: Interaction Between the Acoustic Pressure Fluctuations and the Unsteady Flow Field Through Circular Holes. Journal of Engineering for Gas Turbines and Power 132 (2010), 061501–1–061501–9

[9] Möser, M.: Technische Akustik. Springer, Berlin, Heidelberg, New York, 2007

[10] Bechert, D. W.: Sound absorption caused by vorticity shedding, demonstrated with a jet flow. Journal of Sound and Vibration 70 (1980), 389–405

[11] Haufe, D. et al.: Spectral analysis of the flow sound interaction at a bias flow liner. Applied Acoustics 81 (2014), 47–49